SLAC-PUB-10008
June 2003

Microstructure and Properties of Ultra-Thin Amorphous Silicon Nitride Protective Coating

Bing K. Yen *et al.*

Stanford Linear Accelerator Center, Stanford University, Stanford, CA 94309

Work supported by Department of Energy contract DE–AC03–76SF00515.

Microstructure and properties of ultra-thin amorphous silicon nitride protective coating

Bing K. Yen[a,b)]

IBM Research Division, Almaden Research Center, 650 Harry Road, San Jose, CA 95120

Richard L. White[c)] and Robert J. Waltman[c)]

IBM Storage Technology Division, 5600 Cottle Road, San Jose, CA 95193

Qing Dai,[b)] Dolores C. Miller, Andrew J. Kellock, Bruno Marchon,[b)] and Paul H. Kasai

IBM Research Division, Almaden Research Center, 650 Harry Road, San Jose, CA 95120

Michael F. Toney

Stanford Synchrotron Radiation Laboratory, Stanford Linear Accelerator Center, 2575 Sand Hill Road, M/S 69, Menlo Park, CA 94025

Brian R. York,[c)] Hong Deng,[c)] Qi-Fan Xiao,[c)] and Vedantham Raman[c)]

IBM Storage Technology Division, 5600 Cottle Road, San Jose, CA 95193

ABSTRACT

The effect of N content on the structure and properties of rf reactively sputtered *a*-SiN_x has been studied by Rutherford backscattering spectrometry (RBS), x-ray reflectivity (XRR), ellipsometry, and nano-indentation. The N content in the film increased with the N_2 concentration in the sputtering gas until the Si_3N_4 stoichiometry was reached. The hardness of *a*-SiN_x increased with density, which in turn increased with the N content. The maximum hardness of 25 GPa and density of 3.2 g/cm^3 were attained at the stoichiometric Si_3N_4 composition. With the application of protective overcoat for magnetic disks in mind, thin *a*-SiN_x films were deposited on CoPtCr media to examine their coverage, pinhole density, and wear resistance. According to x-ray photoelectron spectroscopy (XPS), the minimum thickness of *a*-SiN_x required to protect the CoPtCr alloy from oxidation was 10 Å, which was 10 Å thinner than that of the reference *a*-CN_x. A statistic model showed the lower coverage limit of *a*-SiN_x can be attributed to its high density, which corresponds to 93% bulk density of Si_3N_4. Compared with 45 Å *a*-CN_x coated disks, 15 Å *a*-SiN_x coated disks had lower pinhole defect density and superior wear resistance.

[a)] Electronic mail: bing.yen@hgst.com
[b)] Present address: Hitachi Global Storage Technologies, San Jose Research Center, 650 Harry Road, San Jose CA 95120.
[c)] Present address: Hitachi Global Storage Technologies, 5600 Cottle Road, San Jose, CA 95193.

I. INTRODUCTION

In current magnetic disk drive technology, data are written and retrieved by a head, which comprises a magnetic transducer and a sensor, flying hydrodynamically on the disk surface at a height of 10-20 nm. The head and disk surfaces are usually coated with a layer of diamond-like carbon (DLC) to minimize wear and corrosion thereof. Additionally, the DLC overcoat on the disk is covered with a thin layer (~1 nm) of perfluoropolyether (PFPE) lubricant to improve the reliability. The amorphous DLC overcoat, which may be doped with H and/or N, is deposited by sputtering, plasma-enhanced chemical vapor deposition (PECVD), or ion beam deposition (IBD).[1] While DLC films generally provide good wear resistance,[2-3] their structure is porous as evidenced by their relatively low density (1.7-2.1 g/cm^3) compared to that of diamond (3.5 g/cm^3). As the recording density continues to rapidly increase, the simple scaling requirement would necessitate the further reduction of the magnetic spacing between the head and disk and hence the thickness of the protective overcoat. For 1 Tb/in^2 recording density, the magnetic spacing is estimated to be 6.5 nm,[4] and the thickness of the disk overcoat would thus be less than 2 nm by scaling accordingly. A recent study has found, however, that a minimum thickness of approximately 2 nm is required for DLC to fully cover the underlying magnetic layer,[5] which represents a fundamental limitation in using DLC as an ultra thin overcoat in high-density recording.

Silicon nitride (Si_3N_4) is a dense refractory ceramic material known for its superior mechanical properties and chemical inertness owing to its highly oriented covalent bonds. More importantly, it is one of few ceramics that do not catalytically degrade the PFPE lubricant on the disk surface.[6] In the Si_3N_4 structure, each Si atom is surrounded by four neighboring N atoms roughly positioned at the tetrahedral vertices and each N atom is surrounded by three Si atoms situated at the trigonal vertices. Silicon nitride is commonly used in wear resistant applications, such as high speed ball bearings and cutting tool inserts. Silicon nitride can also be deposited as films by chemical vapor deposition (CVD) or sputtering.[7-19] By controlling reactant gas flow rates and other parameters, resultant films (SiN_x) can have a wide range of nitrogen compositions, including the Si_3N_4 stoichiometry.[7-10] Moreover, they are generally amorphous at deposition temperatures of 800 °C and below. Amorphous silicon nitride (a-SiN_x) films can retain local Si-N bonding configurations but lack long-term translational order. Because of their dense film structure, which can

effectively prevent the diffusion of water, oxygen, and even small anions such as Na^+, stoichiometric *a*-SiN_x films are widely used in the IC industry as passivation layers. The film's wear resistance, chemical inertness, and barrier property thus make silicon nitride an ideal protective overcoat for thin-film disks in magnetic disk drives.[11]

Depending on the deposition temperature and film property criteria, *a*-SiN_x films can be deposited by several methods, including atomic-layer deposition (ALD),[12] low-pressure chemical vapor deposition (LPCVD),[7] PECVD,[7,8,11,13-17] and sputtering.[18,19] Amorphous SiN_x films deposited by LPCVD, which typically entails the thermal decomposition of SiH_4 and NH_3 at 800-900 °C, contain little H and hence have a dense structure.[7] By comparison, PECVD utilizes the glow-discharge decomposition of SiH_4 and NH_3 at lower temperatures (300-450 °C) to produce nitride films that still contain significant amount of hydrogen (*a*-SiN_x:H), which increases the porosity of the film.[7,14,17] Studies on *a*-SiN_x:H have shown that their properties critically depend on the H content, which in turn, is influenced by the deposition temperature.[14,17] The density of PECVD nitride films approaches that of LPCVD films only at 400 °C and above,[17] temperatures that are considered too high for the deposition of magnetic media. Hence, sputtering is the only viable way of depositing dense *a*-SiN_x on magnetic disks. While there are several papers on the processing and characterization of PECVD *a*-SiN_x:H,[7,8,11,13-17] few studies have been published on sputtered *a*-SiN_x.[18,19] Sugimoto *et al* have found that near stoichiometric SiN_x films deposited by rf-reactive sputtering at pressures of 4 mTorr and above contained significant amounts of H and O contaminants,[18] which markedly increased etch rates of these films. Such contamination could be effectively minimized by applying a substrate bias during sputtering.[19] To effectively use *a*-SiN_x as a magnetic disk overcoat requires an understanding of the relationship between microstructure and mechanical properties. However, except for the work of Taylor that examines the hardness of select PECVD and LPCVD nitride films,[7] most aforementioned studies focus primarily on optical and electrical properties.[8,12,13,15-17,19,20] The aim of this work was to systematically study the effect of N content in sputtered *a*-SiN_x on its density and hardness, which directly influence the wear and corrosion resistance of *a*-SiN_x overcoats. Ultra-thin *a*-SiN_x (15 Å) was also deposited on magnetic disks to study its performance relative to that of the reference DLC coated disks.

II. EXPERIMENTAL DETAILS

A. Film deposition

Silicon nitride films were deposited using a BPS Circulus M12T static sputtering system equipped with radio frequency (rf) powered (13.56 MHz) cathodes. The base pressure of the sputtering chamber was less than 2×10^{-7} Torr. The rf-reactive sputtering process was carried out using Si targets (99.99% purity) in N_2/Ar atmospheres at 3 mTorr. Nitrogen and argon gases were introduced into the sputtering chamber via a set of mass flow controllers, which can be adjusted to control the N_2 partial pressure in the working gas mixture. The rf power density on the Si target was kept constant at 5.7 W/cm^2. Substrate bias was not applied and the substrate potential was allowed to float during deposition. Thick *a*-SiN_x films (500-1500 Å) were deposited on Si or glass substrates without intentional heating to characterize their intrinsic physical and chemical properties.

B. Film characterization

The chemical composition of 500-1400 Å thick *a*-SiN_x films was determined by a combination of Rutherford Backscattering Spectrometry (RBS) and Forward Recoil Spectrometry (FRS) using a 2.3 MeV He^+ beam from an NEC 3UH Pelletron. The Si and N contents were determined by RBS, and the H content was determined by FRS. RBS data were collected using a detector angle of 170 degrees and a sample tilt of 7 degrees. The beam current was 40 nA and the collected charge was 60 μC per sample. For FRS the sample was tilted to 75 degrees, with a detector angle of 30 degrees. The beam current was 20 nA and the collected charge was 20 μC. A 7 μm aluminum stopper foil was used on the detector to absorb forward scattered He ions. The concentration uncertainty was ± 3 atomic percent for Si and N, and ± 0.5 atomic percent for H. Since several studies have reported the dependence of *a*-SiN_x refractive index on its chemical composition,[8,16] a Rudolph AutoEL ellipsometer is used to measure the refractive indices of film samples at 633 nm wavelength.

Density and thickness of *a*-SiN_x same film samples were determined by x-ray reflectivity (XRR). The specular XRR is analogous to optical reflectivity.[21] At x-ray energies, however, the refractive index, n, becomes slightly less than unity, and $1 - n$ is proportional to the electron density,[22,23] and hence mass density. The refractive index can be expressed as[21]

$$n = 1 - \delta - i\beta \qquad (1)$$

where

$$\delta = \frac{e^2\lambda^2}{2\pi mc^2} N_0 \frac{\rho(Z+f')}{A}$$

and

$$\beta = \frac{\lambda\mu}{4\pi}$$

Here N_0 is Avogadro's number, Z is the average atomic number, A is the average atomic mass, ρ is the mass density, f' is the real part of the anomalous scattering factor, μ is the linear absorption coefficient, and λ is the x-ray wavelength. Since a film always has top and bottom interfaces, interference between x-rays reflected at these interfaces results in an oscillatory pattern similar to optical interference fringes, with the oscillation period inversely proportional to the film thickness. For x-rays that are incident from a medium with refractive index n onto a medium with refractive index n', as shown in Fig. 1, the specular reflectivity R can be described by the Fresnel laws of classical optics $R = R_F = |r_F|^2$,[24] where the Fresnel reflection amplitude is

$$r_F = \frac{\alpha - \left[\alpha^2 - \alpha_c^2 + i(\beta' - \beta)\right]^{1/2}}{\alpha + \left[\alpha^2 - \alpha_c^2 + i(\beta' - \beta)\right]^{1/2}} \qquad (2)$$

Here α is the incidence angle of the x-ray and $\alpha_c = \sqrt{2(\delta' - \delta)}$ is the critical angle for total external reflection. Above the critical angle the reflectivity drops quickly. In this work, the film density is determined from both the critical angle and the amplitude of the oscillation fringes. The specular XRR data was acquired using a BEDE GXR1 X-ray Reflectometer equipped with a (110)-Ge channel-cut beam conditioner and a 50 micron slit aperture that blocks the Cu $K\alpha 2$ line without a post secondary monochromator. The beam divergence was less than 25 arc-seconds (0.00694°) and the samples were aligned to within 5 arc-second. The data was analyzed using the Bede-Refs Mercury program allowing the density,

roughness, and thickness to vary with a figure-of-merit function equal to the absolute value of the difference in the logarithms between the layer-model calculation and the measured intensity. The estimated uncertainties in density and thickness were about ± 0.05 g/cm^3 and ± 1 Å, respectively.

The film hardness was measured by a MTS Nanoinstruments nanoindenter operating in the continuous stiffness mode. With this technique, the stiffness of the Berkovitch indenter contact could be determined continuously during the indenter-loading phase of the test. From these data the projected area of the loaded indenter area were determined, which in combination with the indenter load, provided a continuous measure of both hardness and elastic modulus. The relationship between the indenter area and depth was determined by independent measurements of a fused quartz calibration standard. All *a*-SiN_x films used in hardness measurements were approximately 1200 Å thick. The reported maximum hardness values typically occurred at indentation depths of ~300 Å.

Stress measurements on ~100 Å thick *a*-SiN_x films deposited on 19 mm thick [111] Si wafers were made using a Flexus thin film stress measuring apparatus. This analysis tool measures the radius of curvature of the Si wafer both before and after film deposition. The stress in the deposited film is then calculated using the Stoney equation:[25]

$$\sigma = \frac{Eh^2}{6Rt(1-\nu)}, \qquad (3)$$

where E and ν are the Young's modulus and Poisson's ratio of the substrate, respectively; h and t are the substrate and film thickness, respectively; and R is the change in the radius of curvature of the substrate after the film deposition.

C. Characterization of *a*-SiN_x coated magnetic disks

With the application of *a*-SiN_x as a disk protective overcoat in mind, thin *a*-SiN_x films (less than 25 Å) were deposited on CoPtCr-based magnetic media at 170-190 °C to evaluate their corrosion and wear resistance by comparing to reference media coated with sputtered *a*-CN_x that contains ~10 at.% N. Since the deposition of CoPtCr magnetic alloy requires relatively high deposition temperatures (>200 °C), magnetic disks can exit the sputtering tool at temperatures well above 150 °C. As such, the surface of CoPtCr magnetic

alloy will readily oxide and form a layer of metal oxide in ambient air without the protection of the overcoat. The minimum thickness of overcoat required to protect the CoPtCr alloy from oxidation represents the critical coverage limit, which can be determined by x-ray photoelectron spectroscopy (XPS).[5] Thin *a*-SiN_x and reference *a*-CN_x coated magnetic disks were analyzed by XPS using a Surface Science Instruments SSX-100 ESCA spectrometer with a monochromatic Al $K\alpha$ source. Electron takeoff angle was 37 degrees; a 1 mm spot was used. High resolution (50 eV pass energy, 0.16 eV/step) spectra were taken for carbon (1*s*), oxygen (1*s*), nitrogen (1*s*), silicon (2*p* and 2*s*), cobalt (2*p*), chromium (2*p*) and platinum (4*f*). Binding energies were referenced to $E_{Fermi} = 0$ eV.

The corrosion resistance of magnetic disks depends on the pinhole density of the overcoat, which can be determined by an etch test. The etchant used contained 3% $Ce(NH_4)_2(NO_3)_6$ and 97% H_2O by weight and attacks the underlying CoPtCr alloy. After immersing in the etchant for 3 minutes, *a*-SiN_x and *a*-CN_x coated magnetic disks were examined under an optical microscope.

The tribological performance of magnetic disks depends not only on the wear resistance of the overcoat itself, but also on the interaction between the overcoat and lubricant. The effect of lubricant bonding has been cited as one of the factors that influence the long term reliability of magnetic disks.[26] Therefore, the bonding kinetics of several common perfluoropolyether lubricants on *a*-SiN_x and reference *a*-CN_x coated disks were examined. The perfluoropolyether (PFPE) lubricants used in this work were obtained from Ausimont under the tradenames Zdol 4000, Z-Tetraol 2200, and Zdol-TX 2200. The lubricants were applied to the disks from HFE-7100 solvent using the dip-coat method. For the kinetics studies, all disks were coated with an initial film thickness of 12.0-14.0 Å. The changes in the bonded quantities of the lubricants were measured as a function of time under ambient conditions, 21 °C and nominally 50 ± 10 % relative humidity. The lubricant retained by the disk following a solvent extraction (HFE-7100 and/or Vertrel-XF) is defined as the amount "bonded", which is normalized to the initial film thickness applied to the disk. We note that our use of the term "bonded" lubricant follows the convention historically utilized in the data storage community to describe the fraction of lubricant more tightly adhered to the carbon surface, but it does not necessarily imply chemisorption.

The reliability of the head/disk interface can be evaluated by flying a head continuously over the disk surface. In principle, there should be a clearance of several nanometers between the head and disk under normal operating conditions. In practice, however, the head often makes intermittent contact with the disk while flying. To evaluate the robustness of the head/disk interface, *a*-SiN_x and reference *a*-CN_x disks coated with 10 Å of a PFPE lubricant were subjected to an accelerated flyability test, which entails the flying of a head over the disk surface at a sub-ambient pressure 25 kPa. The low atmospheric pressure ensured the continuous contact between the head and disk. During the test, the head was kept flying on a single track at a velocity of 19 m/s. The acoustic emission signal arose from the rubbing between the head and disk was also monitored. The test was effectively terminated when substantial wear occurs on the head and/or disk surface, causing the head to plough into the disk surface.

III. RESULTS AND DISCUSSION

A. Effect of processing parameters on *a*-SiN_x film composition and properties

Figure 2 shows the RBS spectra of *a*-SiN_x films deposited with different N_2 concentrations in the sputtering gas. The film samples were deposited on glass substrates that had been previously coated with CoPtCr magnetic layers, as evidenced by the Co/Cr and Pt peaks in the spectra. Expectedly, the N/Si peak ratio increases as the N_2 concentration increases from 19 to 38%. To accurately measure the Si and N peak areas, however, the scattered background from the glass substrate is removed. This is achieved by taking a spectrum of a bare glass substrate and subtracting this signal from the spectra of the coated disks. The FRS spectra of the same films reveal that there is only a small amount H in these films and that the H peaks increase in intensity toward the sample surface, which indicates that the H measured is mostly from surface adsorbate contamination such as water or hydrocarbons. Table I summarizes the effect of the N_2 concentration in the sputtering gas on the chemical composition, which is determined by the ratio of the Si, N, and H peak areas from the RBS and FRS spectra. The N content in the *a*-SiN_x film increases with increasing N_2 concentration until the Si_3N_4 stoichiometric composition is reached at the N_2 gas concentration of 33%, beyond which the N content becomes saturated. The N content in *a*-SiN_x films normally ranges from N-deficient to stoichiometric because the formation of N-

rich a-SiN_x would require the creation of N-N or N=N bond, neither of which is thermodynamically stable compared with N≡N. However, N-rich nitride could form under certain conditions: the removal of Si in the film by preferential resputtering and N implantation owing to the substrate bias,[19] the presence of a third element, such as H, that could react with N,[14] and the trapping of N_2 molecules in films. In some a-SiN_x:H films produced by the glow-discharge decomposition of SiH_4 and NH_3, the N/Si ratio can be as high as 2 compared with the stoichiometric ratio of 1.33,[14] because of the formation of excess N-H bonds in the structure. Table I also shows that the H content in films varies between 0.5 and 2.5 at. % and that it decreases with increasing sample thickness, which is consistent with the previous observation that the H measured is mostly from surface adsorbate contamination.

The XRR data of a stoichiometric nitride film deposited on the glass substrate is shown in Fig. 3 along with a fitted curve. The reflected intensity is measured as a function of α and is plotted as a function of the scattering vector Q or $4\pi \sin\alpha / \lambda$. The decay in oscillation amplitude with Q is due to the interfacial roughness with higher roughness causing a faster decrease in the oscillation amplitude. The oscillations, caused by the interference within the a-SiN_x film, have a period of $\Delta Q = 0.011$ Å^{-1}, which corresponds to a thickness of $d = 2\pi / \Delta Q = 575$ Å. Figure 3 also shows that the reflected intensity initially remains constant until reaching the critical angle for total external reflection (α_c), beyond which the intensity markedly drops. Using Eqs. (1) and (2), we can determine the mass density of the particular a-SiN_x film from the measured α_c to be 3.2 g/cm^3. Alternatively, the film density, as well as the thickness and roughness, can be obtained by fitting the entire data range as described in the previous section, which also gives a density value of 3.2 g/cm^3. The fact that these values are the same provides a check of our experimental methodology and gives us great confidence in the accuracy of the film densities.

Figure 4 shows the variation of mass density of a-SiN_x, as determined by XRR, with the N_2 concentration in the sputtering gas. The film density increases with N_2 and asymptotically approaches 3.2 g/cm^3 as the film composition becomes stoichiometric at N_2 gas concentrations of 33% and higher. At the maximum N_2 gas concentration of 51%, however, the film density apparently drops to 3.05 g/cm^3. This suggests that the sputtered film becomes more porous at the maximum N_2 concentration since its chemical composition

remains essentially stoichiometric (Table I). Interestingly, while the Si atomic density of Si_3N_4 is similar to that of Si, the overall mass density of Si_3N_4 (3.44 g/cm^3) is 50% higher than that of Si (2.33 g/cm^3). The Si or SiN_x structure is densified with N incorporation, which replaces the Si-Si bond (2.4 Å) with stronger and shorter Si-N bond (1.7 Å),[27] until the Si_3N_4 stoichiometry is reached, as illustrated in Fig. 5. The stoichiometric *a*-SiN_x has a maximum density of 3.2 g/cm^3, which is equivalent to 93% bulk density of Si_3N_4. The mass density values of silicon nitride films deposited by low-pressure chemical vapor deposition (LPCVD) and plasma-enhanced chemical vapor deposition (PECVD) are also shown for comparison.[7] The PECVD *a*-SiN_x:H films produced by the glow-discharge decomposition of SiH_4 and NH_3 could contain significant amounts of H (10-25 at.%) because of the relatively low deposition temperature (less than 400 °C) involved.[7,8,11,13-17] The formation of Si-H and N-H in *a*-SiN_x:H at low temperatures effectively terminates the 3-dimensional bonding network and thus reduces the density. By contrast, *a*-SiN_x deposited by LPCVD, which typically entails the thermal decomposition of SiH_4 and NH_3 at 800-900 °C, and *a*-SiN_x deposited by rf-reactive sputtering contain little H and are considerably denser than PECVD *a*-SiN_x:H.

The refractive index (*n*) of *a*-SiN_x as a function of the N_2 concentration in the sputtering gas is shown in Fig. 6. For reference purpose, the N/Si ratio is also plotted in the same figure. The refractive index initially falls as the N content in *a*-SiN_x increases. It then asymptotically approaches 1.98 as N/Si reaches the stoichiometric ratio of 1.33. All stoichiometric *a*-SiN_x film samples have a refractive index of 2.00 ± 0.02 at 633 nm, which is comparable to that of dense LPCVD nitride (1.98-2.02).[18] The relationship between the refractive index and the N content in the film is clearly illustrated in Fig. 7. The refractive index decreases linearly with the N content, which is in good agreement with those of sputtered *a*-SiN_x films produced by Davis *et al* shown in the same figure.[8] This result should also be applicable to LPCVD *a*-SiN_x that contains negligible H. While ellipsometry can be a practical method for determining the chemical composition of silicon nitride films, one should be aware that the refractive index depends not only on the N content, but also the presence of other elements, such as H and O. Moreover, it tends to decrease with increasing film porosity. Figure 7 also shows the results of other works on PECVD *a*-SiN_x:H, which contained several atomic percent hydrogen. Comparing with hydrogen-free *a*-SiN_x, *a*-

SiN_x:H has consistently lower refractive index at a given N content or N/Si ratio. This may be partly due to the formation of Si-H and N-H bonds, which effectively disrupt the network of Si-N bonds and decreases the film density. Accordingly, the refractive index of silicon nitride decreases with increasing H content. Most PECVD nitrides have a refractive index of 1.6-1.9, depending on the H content.[8] The incorporation of oxygen in silicon nitride, whether through doping or contamination, can also markedly decrease the refractive index, because silicon oxide has a lower refractive index (~1.45). This knowledge is effectively utilized in the fabrication of optical waveguides, which use SiO_xN_y and SiO_x to provide a high contrast of the refractive index.[28,29]

Figure 8 shows the hardness and residual stress of *a*-SiN_x as functions of the N_2 concentration in the sputtering gas. The hardness value initially increases with the N_2 concentration as N is incorporated into the *a*-SiN_x film. It then reaches an asymptotic value of approximately 25 GPa at 33% N_2, the point at which the film composition becomes stoichiometric. The increase in hardness is accompanied by a concomitant decrease in the residual compressive stress, which is in contrast to the results of Kim and Chung.[19] Their sputtered *a*-SiN_x is densified by physical ion bombardment that normally induces higher residual compressive stress, whereas the hardness and residual stress of current *a*-SiN_x films are governed by their chemical composition and hence chemical bonds. While the current work shows the residual stress of *a*-SiN_x becoming increasingly tensile with N incorporation, another study has found that the residual stress of *a*-SiN_x:H becomes increasingly compressive with N incorporation owing to the extensive formation of N-H bonds.[7] The relationship between hardness and density for *a*-SiN_x is illustrated in Fig. 9, which also includes data from LPCVD and PECVD nitrides for comparison.[7] The hardness of nitrides apparently increases with density, which in turn increases with the N content as shown previously in Fig. 5. Stoichiometric *a*-SiN_x deposited by LPCVD or sputtering has higher hardness (23-25 GPa) than that of PECVD *a*-SiN_x:H (16-20 GPa) because the former has higher density. Accordingly, results on *a*-SiN_x coated disks in the following section are limited to sputtered stoichiometric *a*-SiN_x, which has a maximum density of 3.2 g/cm^3 and a hardness of 25 GPa.

B. Coverage and properties of *a*-SiN_x coated magnetic disks

One of the requirements for ultra-thin overcoat is the ability of the film to fully cover the underlying surface at low thickness. The minimum thickness required for such coverage, which depends on film properties as well as the topography of the underlying surface, represents a fundamental limit on the overcoat thickness. The coverage of overcoat on magnetic disks can be studied by x-ray photoelectron spectroscopy (XPS) because the surface of CoPtCr magnetic media will readily oxidize in air without the protective overcoat.[5] The XPS result in Fig. 10(a) shows the evolution of the Co2*p* core level spectrum with the overcoat thickness for *a*-SiN_x coated disks. The Co2*p* spectrum of the bare magnetic disk consists of a single peak at ~780 eV, which can be attributed to Co oxide.[5] This suggests that 3-5 nm of Co oxide is formed on the surface of the CoPtCr without the overcoat protection. When 5 Å of *a*-SiN_x is deposited on the CoPtCr surface, however, the intensity of the Co oxide peak decreases while a second peak at ~778 eV that corresponds to Co metal appears in the spectrum. The 5 Å thick *a*-SiN_x overcoat provides limited protection against oxidation in air as evidenced by the presence of the metal peak. As the thickness of *a*-SiN_x is increased to 10 Å, the oxide peak completely disappears and only the metal peak remains in the Co2*p* spectrum, which indicates that 10 Å of *a*-SiN_x is sufficient to cover the underlying CoPtCr alloy and prevent the oxidation thereof. Further increase in the *a*-SiN_x thickness does not alter the XPS Co2*p* core level spectrum, except for the decrease in the Co metal peak intensity because of the attenuation by thicker *a*-SiN_x.

Comparing with the XPS results of *a*-SiN_x coated disks, Fig. 10(b) shows the XPS Co2*p* core level spectra for the reference *a*-CN_x coated disks. Like the Co2*p* spectrum of the bare CoPtCr alloy, the spectrum of the 11 Å *a*-CN_x exhibits only the metal oxide peak, which indicates that 11 Å thick *a*-CN_x does not provide any protection against oxidation in air. As its thickness increases to 15 Å, *a*-CN_x begin to provide limited protection as evidenced by the presence of Co metal peak. The disappearance of oxide peak at 23 Å implies a complete coverage is attained. Hence, the minimum *a*-CN_x thickness required for coverage can be estimated to be 20 Å, which is in agreement with a previous study.[5] Compared with *a*-CN_x, *a*-SiN_x has a lower coverage limit of only 10 Å. This difference may be partly due to their respective densities. The density of *a*-SiN_x, as determined by XRR in the previous section, is

3.2 g/cm^3, which corresponds to 93% bulk density of Si_3N_4. By contrast, the density of *a*-CN_x, 1.9 g/cm^3, is equivalent to only 54% bulk density of diamond.

To further investigate the effect of relative density, or the ratio of the actual film density to the theoretical density, on the critical coverage thickness of overcoat, a statistic, purely random model of the atomic stacking structure is constructed and compared to the XPS results. First, the relative density of each atomic layer is assumed to be same as the overall relative density of the film. Hence, for a film with n layers of atoms, the fraction of surface without any atoms can be expressed as

$$H_0 = (1-\rho)^n, \tag{4}$$

where ρ is the relative density of the film. Similarly, the fraction of surface with only L layers of atoms can be described by

$$H_L = \frac{n!}{L!(n-L)!}\rho^L(1-\rho)^{n-L} \text{ for } n > L > 0. \tag{5}$$

Therefore, the fraction of surface that is fully covered by at least k layers of atoms is

$$C_k = 1 - H_0 - H_1 \cdots - H_{k-1}$$

or

$$C_k = 1-(1-\rho)^n - \sum_{L=1}^{k-1}\frac{n!}{L!(n-L)!}\rho^L(1-\rho)^{n-L} \quad . \tag{6}$$

Because of the complicated nature of Co oxidation involved and the lack of reference information on the effect of roughness on coverage, it is initially assumed that a finite number k of atomic layers are needed to prevent the oxidation of CoPtCr surface with RMS roughness of 6-8 Å at 170-190 °C. Equation (6) thus describes the film coverage in terms of the relative film density (ρ), the minimum number of layers required to prevent oxidation (k), and the number of total layers (n). Assuming that each atomic layer has a thickness of 1.5 Å for small covalently bonded atoms, the coverage according to Eq. (6) is plotted as a function

of the overcoat thickness in Fig. 11 for ρ = 55-95% and k = 4. Expectedly, the coverage increases more rapidly with overcoat thickness for higher relative density values. The critical coverage thickness, defined here as the thickness at which $C_k \geq 0.99$, for k = 4 (i.e. 4 layers of atoms are required to prevent Co oxidation) can then be plotted as a function of the relative density as shown in Fig. 12. Likewise, critical coverage thickness for different k values is obtained by following the above procedures and is also shown in the same figure. The coverage thickness decreases by ~3 Å, or 2 atomic layers, with every 10% increase in the relative density. The simulation results for k = 4 are in good agreement with the XPS results, which also include that of an *a*-C:H film produced by ion beam deposition.[1] With the assumptions made in the model, this suggests that a minimum of 4 layers of overcoat atoms are required to prevent the oxidation of the CoPtCr surface with RMS roughness of 6-8 Å at 170-190 °C. As the roughness or the oxidation temperature increases, however, the value of k would also expect to increase because more layers of atoms are required to protect the underlying CoPtCr alloy.

Figure 13 shows the surface of 15 Å *a*-SiN_x and 45 Å *a*-CN_x coated disks after immersing in the $Ce(NH_4)_2(NO_3)_6$ solution for 3 minutes. The dark spots represent pinhole defects through which the etchant attacked the underlying CoPtCr magnetic alloy. While there is no visible pinhole on the *a*-SiN_x disk, the surface of the reference *a*-CN_x disk is covered by pinhole defects ($10/cm^2$). The pinhole decoration test clearly demonstrates that the 15 Å *a*-SiN_x film can provide better corrosion protection than the thicker reference *a*-CN_x film. Routine reliability tests in this laboratory have found that 15 Å of *a*-SiN_x is indeed sufficient to protect the underlying CoPtCr alloy from corrosion. However, some researchers recently have reported that 8 nm of sputtered *a*-SiN_x is needed to prevent the underlying CoSm magnetic alloy from corroding.[30] The thicker *a*-SiN_x required may be attributed to the propensity for their CoSm alloys to oxidize and the quality of their *a*-SiN_x film. Compared with CoPtCr alloys, which tends to passivate owing to the presence of Cr, SmCo alloys are highly susceptible to corrosion because of the rare earth Sm constituent. Moreover, their *a*-SiN_x film, sputter-deposited using a Si_3N_4 compound target in a pure Ar atmosphere, is very likely to be Si-rich and hence has a lower density, as demonstrated in the previous section. Their higher sputtering pressure of 5 mTorr could also potentially introduce significant amounts of H and O into the film,[18] which would again effectively decrease the film density.

The ambient bonding kinetics for Zdol 4000, Zdol-TX 2200, and Z-Tetraol 2200 lubricants on *a*-SiN_x and *a*-CN_x and are presented in Fig. 14. Upon application of the lubricants to the overcoat surface, a fraction of the lubricant bonds at room temperature within the time required to allow for solvent evaporation and to conduct the inititial thickness measurements. This quantity of bonded lubricant is referred to as the initial bonded fraction. On both *a*-SiN_x and *a*-CN_x disks, the initial bonded fraction of Z-Tetraol (~60%) is consistently higher that of Zdol-TX, which in turn is higher than that of Zdol. Previous work has shown that the bonding of lubricants to carbon surface may be driven by the decrease in free energy that occurs as a results of the interactions between the polar hydroxyl end groups of the lubricant molecules and the polar functional groups on the carbon surface.[31] Hence, the higher initial bonded fraction of Z-Tetraol is possibly due to the presence of two hydroxyl groups per chain end compared with only one per chain end for Zdol-TX and Zdol. Although both Zdol-TX and Zdol have only one hydroxyl group per chain end, the more flexible Zdol-TX end groups may allow for a more facile spatial delivery of the hydroxyl end group than Zdol to within the capture radius of surface active site owing to a more freely rotating bond.[32] While the initial lubricant bonding results for *a*-SiN_x and *a*-CN_x are similar, the subsequent bonding kinetics (bonding with time) proved to be very different. The amount of bonded lubricant on *a*-SiN_x remains essentially constant with time for all lubricants, whereas the amount on *a*-CN_x increases with time and may be fitted by a stretched exponential for the rate coefficient, $k(t) = k_o t^{-h}$. This difference in the lubricant bonding kinetics may be partly attributed to the difference in the structure of *a*-SiN_x and *a*-CN_x films. A previous electron spin resonance (ESR) study has revealed that thin *a*-CN_x films are porous and contain high concentrations of dangling bonds (~$10^{21}/cm^3$).[33] As lubricant molecules increasingly bond to *a*-CN_x with time, the dangling bond density decreases, indicating that interactions between dangling bonds in *a*-CN_x films and lubricant molecules that gradually diffused into these porous films are partly responsible for the observed bonding kinetics. By contrast, *a*-SiN_x films are dense and they do not contain dangling bonds according to ESR.

The wear resistance of *a*-SiN_x and *a*-CN_x coated disks can be evaluated by flying a recording head continuously over the disk surface at sub-ambient pressure (25 kPa) to ensure continuous contact. Figure 15 shows the acoustic emission (AE) signals from recording

heads flying over 15 Å a-SiN_x and 45 Å a-CN_x disks coated with 10 Å of Z-Tetraol lubricant. Stable AE signals are generated as recording heads rub against disk surface during the test. When the disk overcoat is worn through, however, severe damages to both disk and head surface prevent the stable contact between the head and disk surface, causing the AE signal to fall precipitously. Amorphous SiN_x coated disks last 180-360 min, whereas a-CN_x coated disks last only 50-90 min. Despite the thickness differences, the thinner a-SiN_x overcoat outperforms the thicker a-CN_x overcoat in this accelerated flyability test. The superior wear resistance of a-SiN_x may be partly attributed to its hardness of 25 GPa, which is significantly higher than that of a-CN_x (12 GPa). Since all disks were tested approximately one month after they were initially coated with the lubricant, the fraction of lubricant that is not bonded to the surface, or free lubricant, on a-SiN_x (30%) is higher than that on a-CN_x (20%) as previously shown in Fig. 14. Therefore, it is also possible that the wear resistance of a-SiN_x is enhanced by the presence of more free lubricant.[26]

IV. CONCLUSIONS

The effect of N content on the structure and properties of rf reactively sputtered a-SiN_x has been investigated. The N content in the a-SiN_x film increases with the N_2 flow rate until the stoichiometric composition (Si_3N_4) is reached. The refractive index asymptotically reaches 1.99 as the N/Si ratio approaches 1.33. Because of the linear relationship between the refractive index and the N content in the film, ellipsometry can be a practical technique for determining the chemical composition of a-SiN_x. The hardness of a-SiN_x increases with density, which in turn increases with the N content in the film. The maximum density of 3.2 g/cm^3 and hardness of 25 GPa are attained at the stoichiometric composition. These values are comparable to those of LPCVD a-SiN_x but are significantly higher than those of PECVD a-SiN_x:H.

The XPS results on stoichiometric a-SiN_x coated magnetic disks show that 10 Å of a-SiN_x can effectively protect the underlying CoPtCr magnetic alloy from oxidizing as disks exit the sputtering chamber. This minimum coverage thickness is 10 Å thinner than that of the reference a-CN_x, allowing the recording head to fly potentially closer to the CoPtCr layer. Numerical simulation based on a statistical model reveals that the lower coverage thickness of a-SiN_x can be attributed to its high density (3.2 g/cm^3), which corresponds to 93% bulk

density of Si_3N_4. According to the model, the coverage thickness of overcoat decreases by ~3 Å with every 10% increase in the relative density, which is in good agreement with experimental XPS results. Comparisons between 15 Å *a*-SiN_x and 45 Å reference *a*-CN_x coated disks show thinner *a*-SiN_x actually has fewer pinhole defects and is more durable in the aggressive flyability test. The superior wear resistance of ultra-thin *a*-SiN_x can be attributed to its high hardness and favorable interactions with the lubricant.

ACKNOWLEDGMENTS

The authors gratefully acknowledge Mrs. V. Yra for the pinhole decoration test and Dr. J. Lyerla for his support and encouragement during the course of this work.

REFERENCES

[1] B. K. Yen, J.-U. Thiele, M. Geisler, P. H. Kasai, R. L. White, B. R. York, H. Zadoori, A. J. Kellock, W. C. Tang, T.-W. Wu, M. F. Toney, and B. Marchon, IEEE Trans. Magn. **37**, 1786 (2001).

[2] T.-W. Wu, V. Deline, T. W. Scharf, B. K. Yen, and J. A. Bernard, J. Vac. Sci. Technol. A **19**, 986 (2001).

[3] T. W. Scharf, T.-W. Wu, B. K. Yen, B. Marchon, and J. A. Barnard, IEEE Trans. Magn. **37**, 1792 (2001).

[4] R. W. Wood, J. Miles, and T. Olson, IEEE Trans. Magn. **30**, 1711 (2002).

[5] C. M. Mate, B. K. Yen, D. C. Miller, M. F. Toney, M. Scarpulla, and J. Frommer, IEEE Trans. Magn. **36**, 110 (2000).

[6] R. Koka and F. Armatis, Trib. Trans. 40, 63 (1997).

[7] J. A. Taylor, J. Vac. Sci. Technol. A **9**, 2464 (1991).

[8] E. A. Davis, N. Piggins, and S. C. Bayliss, J. Phys. C **20**, 4415 (1987).

[9] F. C. Stedile, I. J. R. Baumvol, W. H. Schreiner, and F. L. Freire, J. Vac. Sci. Technol. A **10**, 462 (1992).

[10] M. A. Sobolewski and C. R. Helms, J. Vac. Sci. Technol. A **6**, 1358 (1988).

[11] Z. Kovac and V. J. Novotny, IEEE Trans. Magn. **27**, 5071 (1991).

[12] A. Nakajima, T. Yoshimoto, T. Kidera, and S. Yokoyama, Appl. Phys. Lett. **79**, 665 (2001).

[13] J. R. Flemish and R. L. Pfeffer, J. Appl. Phys. **74**, 3277 (1993).

[14] T. M. Klein, T. M. Anderson, A. I. Chowdhury, and G. N. Parsons, J. Vac. Sci. Technol. A **17**, 108 (1999).

[15] J. Vuillod, J. Vac. Sci. Technol. A **5**, 1675 (1987).

[16] H. J. Stein, V. A. Wells, and R. E. Hampy, J. Electrochem. Soc. **126**, 1750 (1979).

[17] M. Arps and A. Markwitz, J. Vac. Sci. Technol. A **15**, 1864 (1997).

[18] I. Sugimoto, K. Yanagisawa, and H. Kuwano, J. Vac. Sci. Technol. A **12**, 2859 (1994).

[19] J. H. Kim and K. W. Chung, J. Appl. Phys. **83**, 5831 (1998).

[20] S. Mirsch and J. Bauer, Phys. Stat. Sol. A **26**, 579 (1974).

[21] M. F. Toney and S. Brennan, J. Appl. Phys. **66**, 1861 (1989).

[22] C. G. Darwin, Philos. Mag. **27**, 315 (1914).

[23] A. H. Compton, Philos. Mag. **45**, 1121 (1923).

[24] M. Born and E. Wolf, *Priciples of Optics* (Pergamon, Oxford, 1970).

[25] G. Stoney, Proc. R. Soc. London A **82**, 172 (1909).

[26] T. E. Karis, G. W. Tyndall, and R. J. Waltman, Trib. Trans. **44**, 249 (2001).

[27] A. A. Korkin, J. V. Cole, D. Sengupta, and J. B. Adams, J. Electrochem. Soc. **146**, 4203 (1999).

[28] R. Germann, H. W. M. Salemink, R. Beyeler, G. L. Bona, F. Horst, and B. J. Offrein, J. Electrochem. Soc. **147**, 2237 (2000).

[29] B. J. Offrein, F. Horst, G. L. Bona, R. Germann, H. W. M. Salemink, and R. Beyeler, IEEE Photonics Technol. Lett. **12**, 504 (2000).

[30] I. Zana and G. Zangari, J. Vac. Sci. Technol. A **19**, 1203 (2001).

[31] R. J. Waltman, G. W. Tyndall, J. Pacansky, and R. J. Berry, Trib. Lett. **7**, 91 (1999).

[32] R. J. Waltman and M. G. Shieh, Macromolec. **34**, 6776 (2001).

[33] P. H. Kasai, A. Wass, and B. K. Yen, J. Info. Storage Proc. Syst. **1**, 245 (1999).

TABLE I. Chemical compositions of *a*-SiN_x films sputtered deposited under different N_2 partial pressures

N_2 in sputtering gas (%)	Si (at. %)	N (at. %)	H (at. %)	Thickness (Å)
19	64.6 ± 3	34.6 ± 3	0.7 ± 0.5	1351
28	48.9 ± 3	50.5 ± 3	0.6 ± 0.5	1242
33	44.8 ± 3	54.4 ± 3	0.8 ± 0.5	951
38	42.6 ± 3	56.1 ± 3	1.2 ± 0.5	693
43	44.3 ± 3	54.0 ± 3	1.6 ± 0.5	575
47	43.0 ± 3	55.1 ± 3	1.9 ± 0.5	552
51	43.7 ± 3	54.1 ± 3	2.2 ± 0.5	504

LIST OF FIGURE CAPTIONS

FIG. 1. X-ray reflectivity geometry.

FIG. 2. RBS spectra of *a*-SiN_x films deposited with different N_2 concentrations in the sputtering gas: (a) 19% N_2, (b) 28% N_2, and (c) 38% N_2.

FIG. 3. XRR spectrum and fitted curve for a stoichiometric *a*-SiN_x film deposited on glass substrate.

FIG. 4. Variation of *a*-SiN_x film density with N_2 concentration in sputtering gas.

FIG. 5. Effect of N content in *a*-SiN_x on film density. LPCVD and PECVD results from Taylor [7] are also shown for comparison.

FIG. 6. Variations of refractive index and N/Si ratio of *a*-SiN_x with N_2 concentration in sputtering gas.

FIG. 7. Effect of N content in *a*-SiN_x on refractive index. Results from Davis *et al* [8] and Stein *et al* [16] are also plotted for comparison.

FIG. 8. Variations of hardness and residual stress of *a*-SiN_x with N_2 concentration in sputtering gas.

FIG. 9. Variation of hardness with mass density for silicon nitride films.

FIG. 10. XPS Co2*p* core level spectra of (a) *a*-SiN_x coated and (b) *a*-CN_x coated CoCrPt disks.

FIG. 11. Effect of overcoat thickness on coverage for various relative density values according to the model described by Eq. (6) with $k = 4$.

FIG. 12. Variation of overcoat coverage thickness with relative density according to simulation and XPS experiments.

FIG. 13. Surfaces of CoPtCr disks coated with (a) 15 Å *a*-SiN_x and (b) 45 Å *a*-CN_x after 3 min etch in $Ce(NH_4)_2(NO_3)_6$ solution.

FIG. 14. Changes in the bonded fractions of Zdol 4000, Zdol-TX 2200, and Z-Tetraol 2200, on (a) *a*-SiN_x and (b) *a*-CN_x coated disks as a function of time at 21 °C and 50 ± 10% relative humidity. The initial lubricant film thicknesses are 13.0 ± 0.5 Å and 12.0 ± 0.5 Å for *a*-SiN_x and *a*-CN_x disks, respectively.

FIG. 15. Sample AE signals recorded during sub-ambient flyability test for (a) 15 Å *a*-SiN_x and (b) 45 Å *a*-CN_x coated disks.

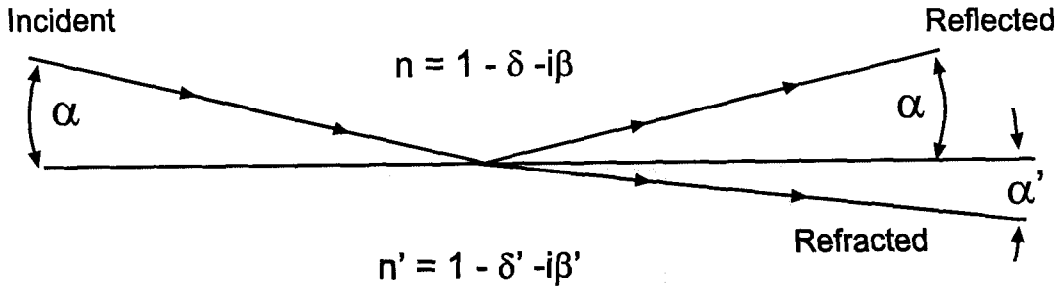

FIG. 1. X-ray reflectivity geometry.

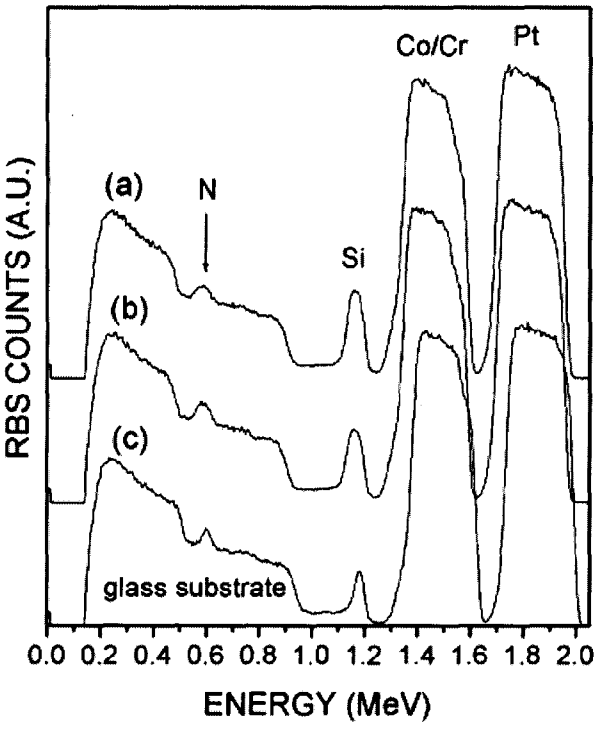

FIG. 2. RBS spectra of *a*-SiN_x films deposited with different N_2 concentrations in the sputtering gas: (a) 19% N_2, (b) 28% N_2, and (c) 38% N_2.

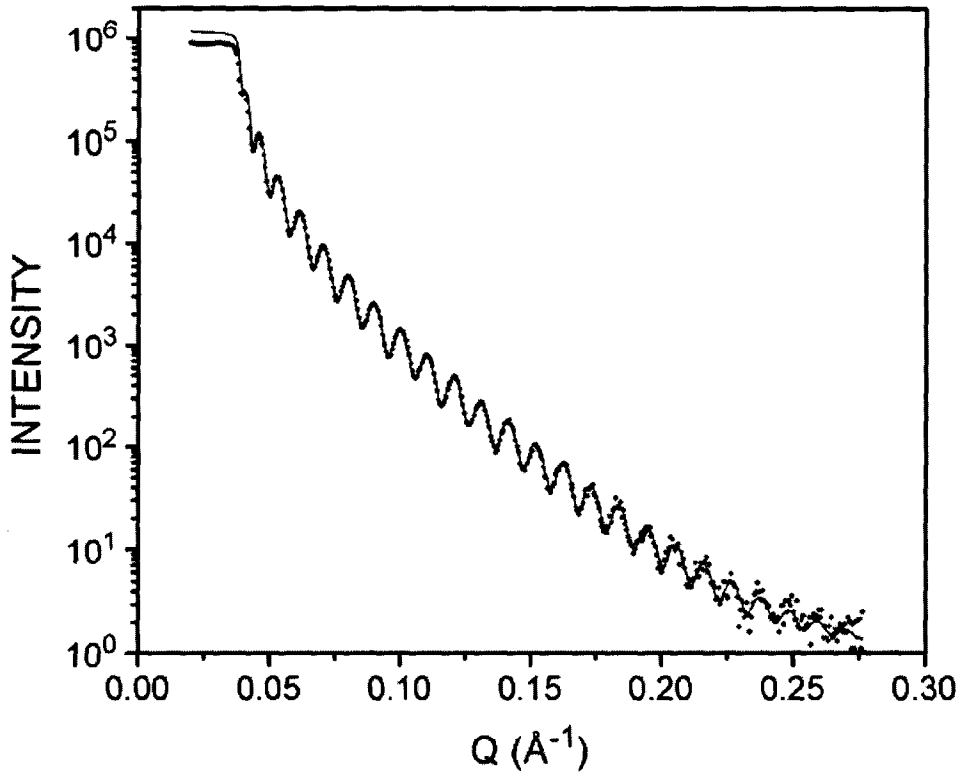

FIG. 3. XRR spectrum and fitted curve for a stoichiometric *a*-SiN_x film deposited on glass substrate.

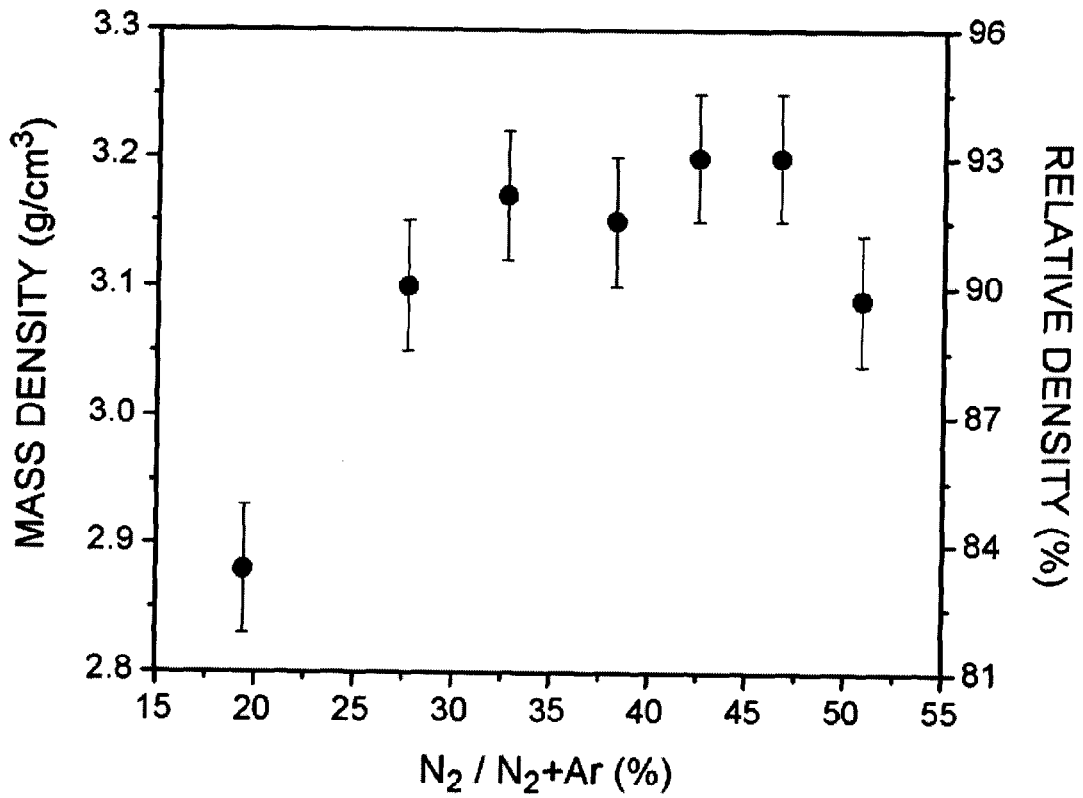

FIG. 4. Variation of a-SiN_x film density with N_2 concentration in sputtering gas.

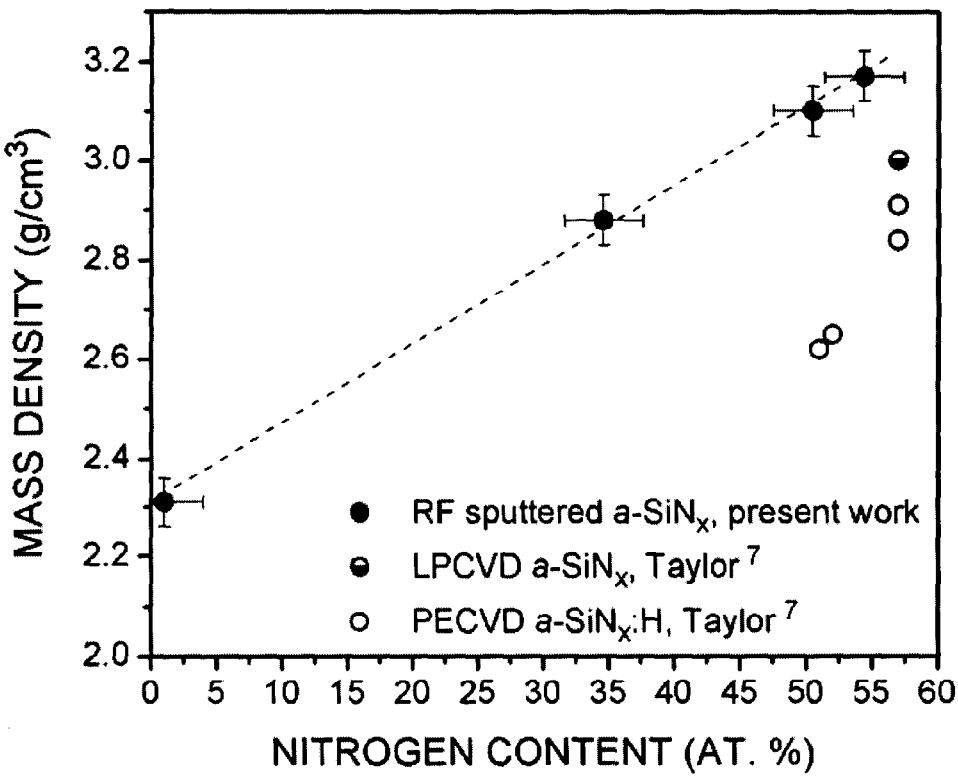

FIG. 5. Effect of N content in a-SiN_x on film density. LPCVD and PECVD results from Taylor [7] are also shown for comparison.

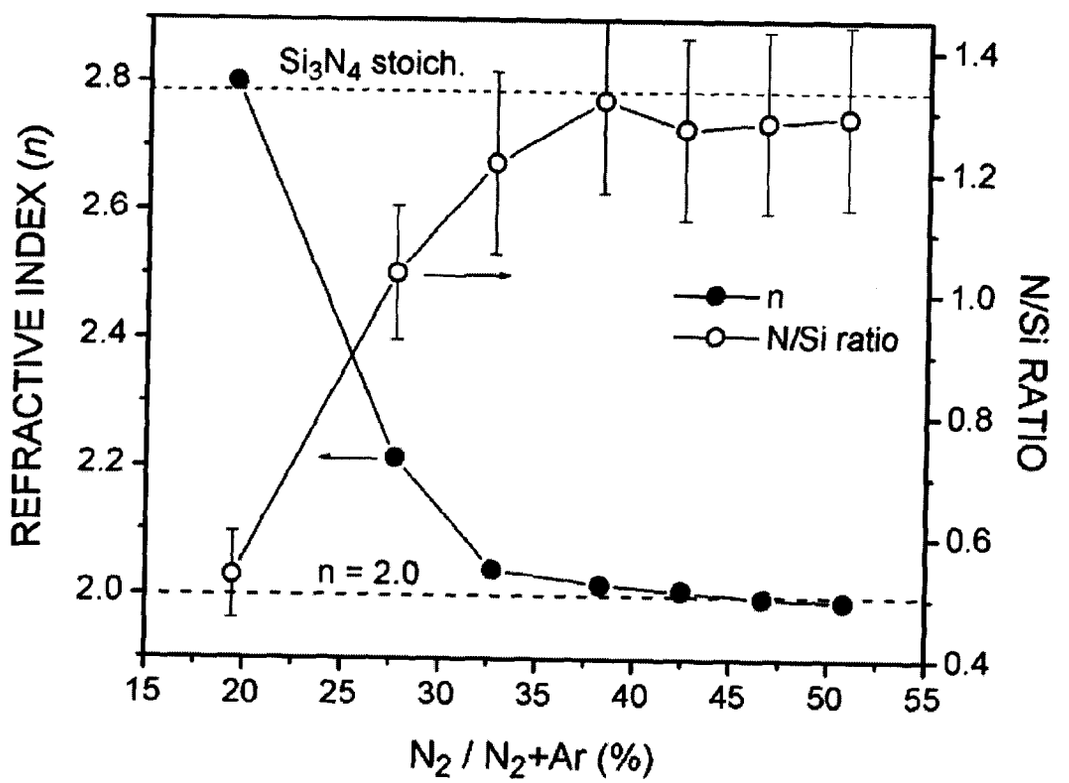

FIG. 6. Variations of refractive index and N/Si ratio of a-SiN_x with N_2 concentration in sputtering gas.

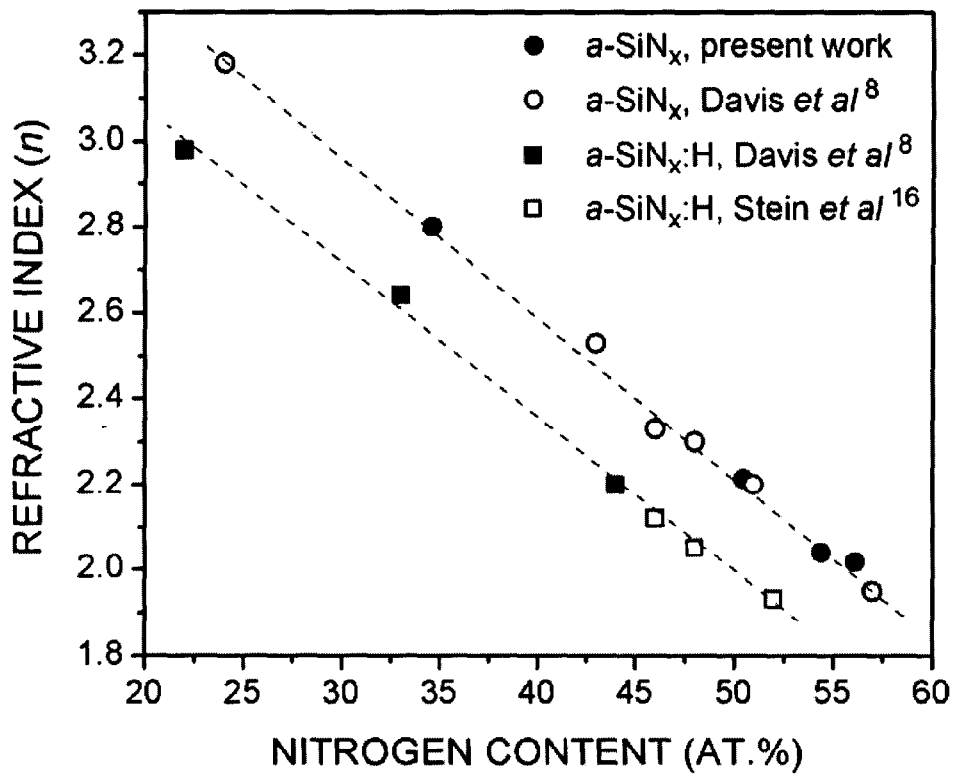

FIG. 7. Effect of N content in a-SiN_x on refractive index. Results from Davis *et al*[8] and Stein *et al*[16] are also plotted for comparison.

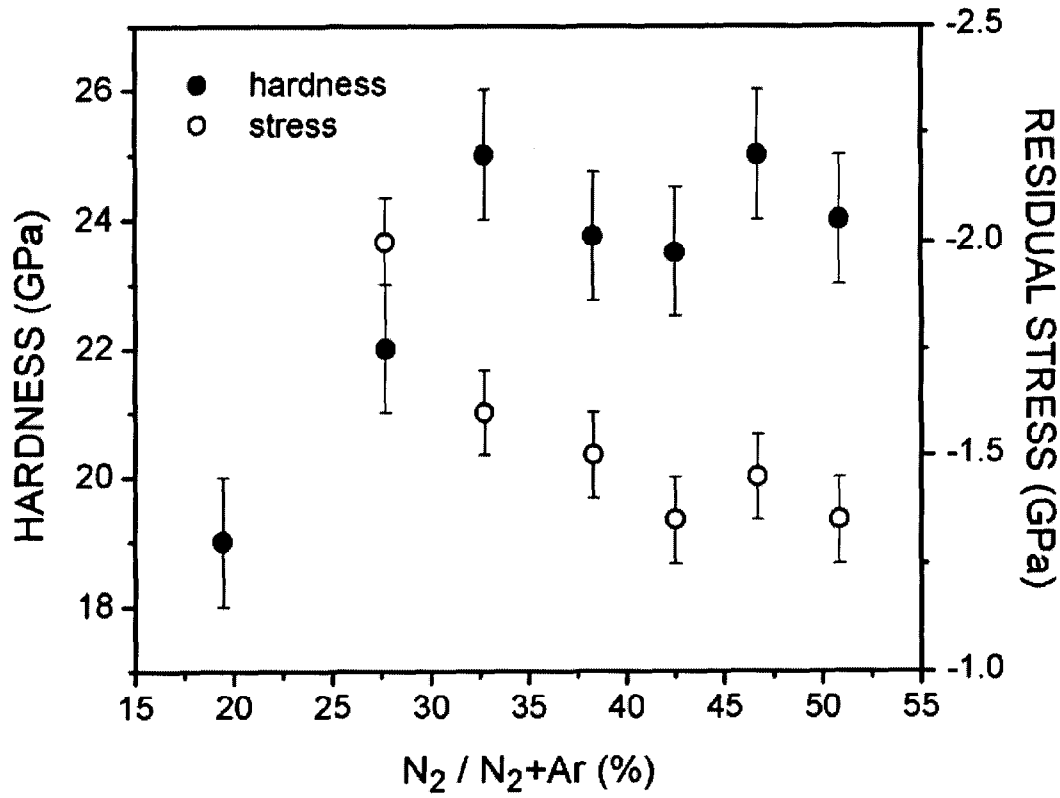

FIG. 8. Variations of hardness and residual stress of a-SiN_x with N_2 concentration in sputtering gas.

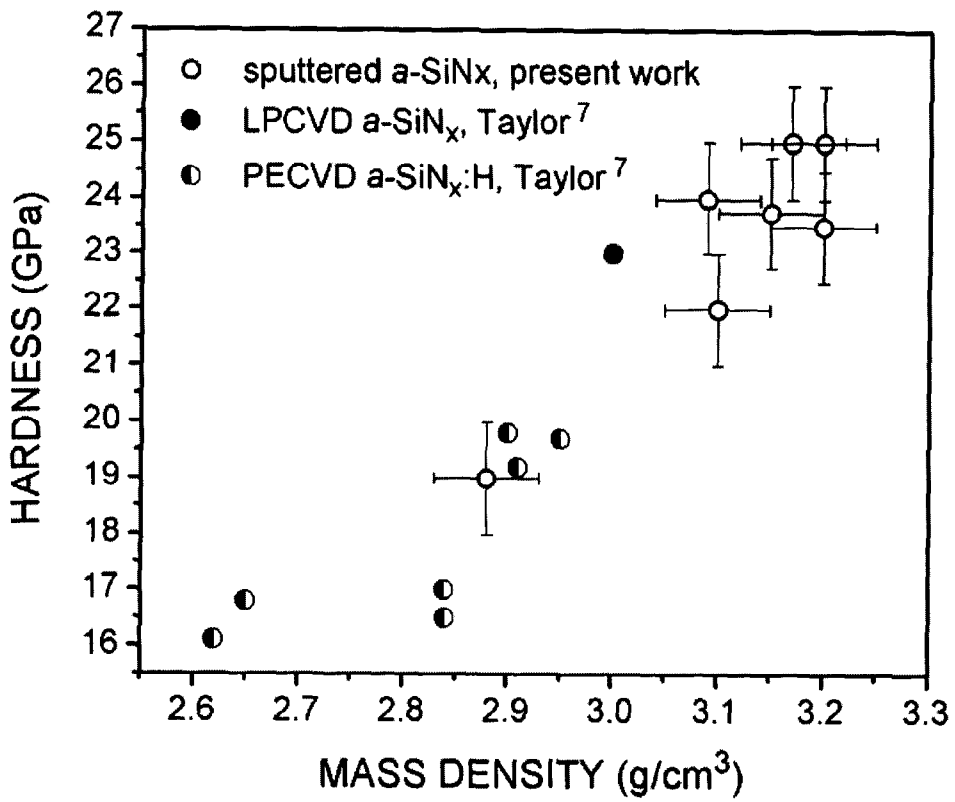

FIG. 9. Variation of hardness with mass density for silicon nitride films.

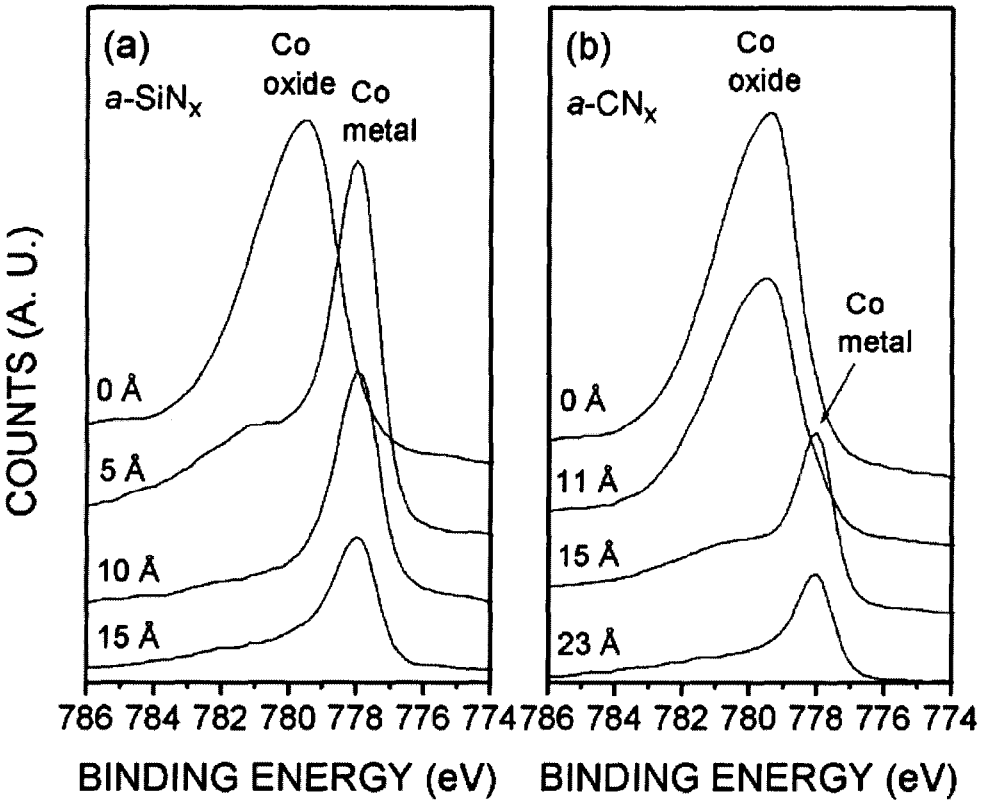

FIG. 10. XPS Co2*p* core level spectra of (a) *a*-SiN_x coated and (b) *a*-CN_x coated CoCrPt disks.

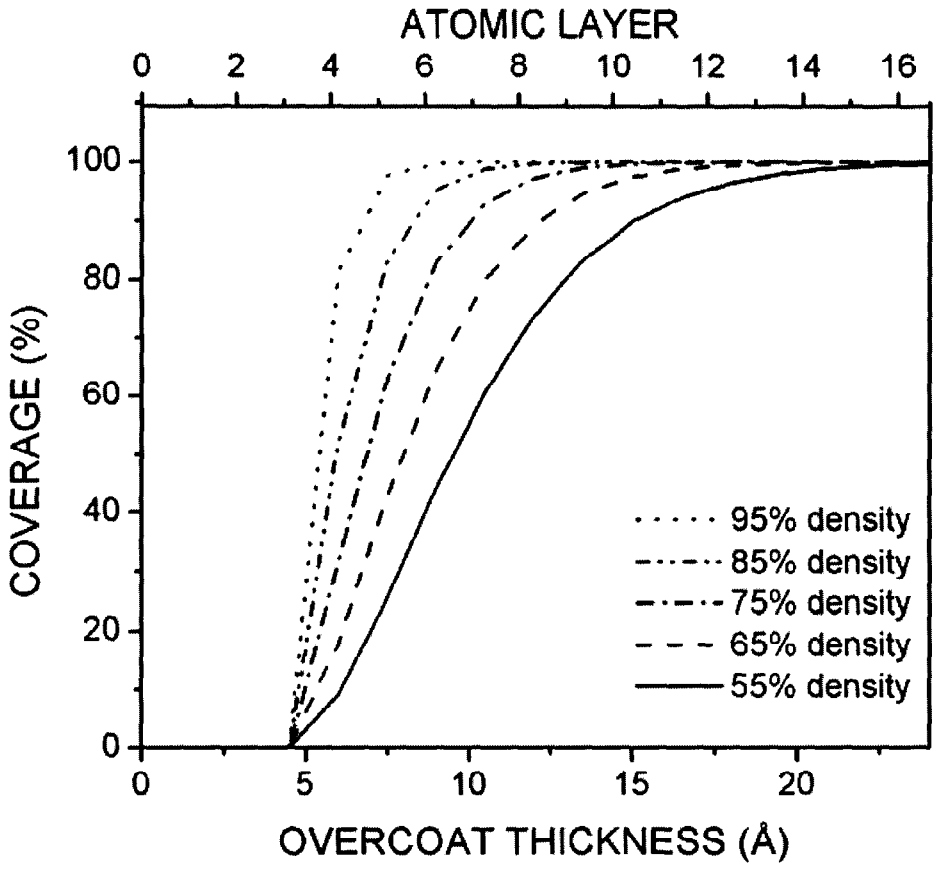

FIG. 11. Effect of overcoat thickness on coverage for various relative density values according to the model described by Eq. (6) with $k = 4$.

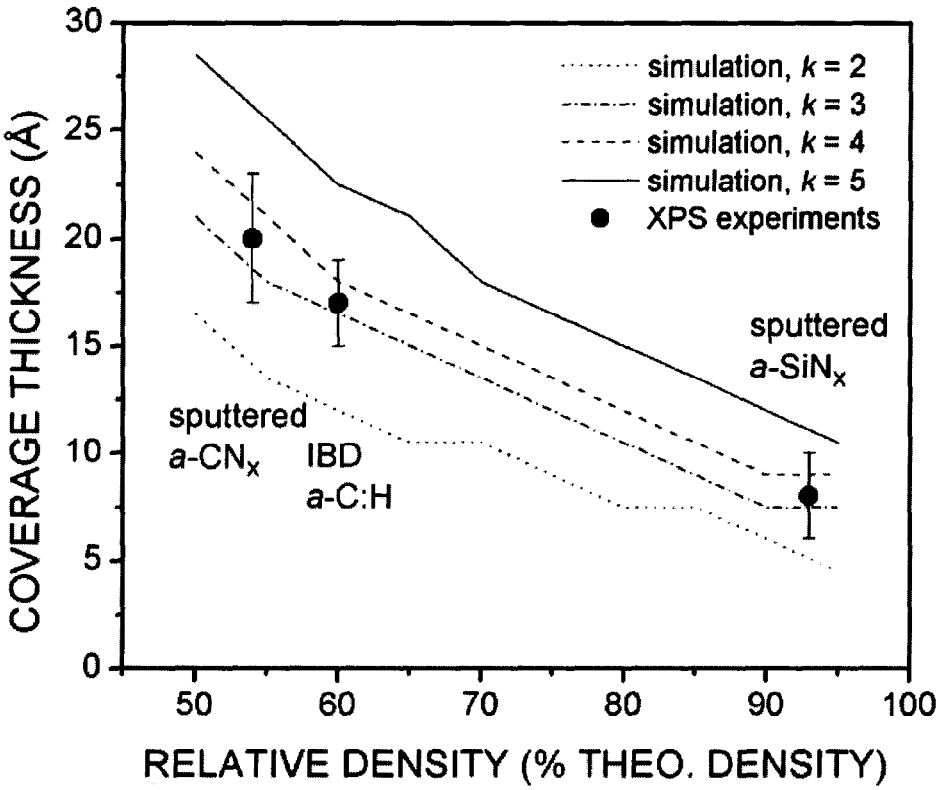

FIG. 12. Variation of overcoat coverage thickness with relative density according to simulation and XPS experiments.

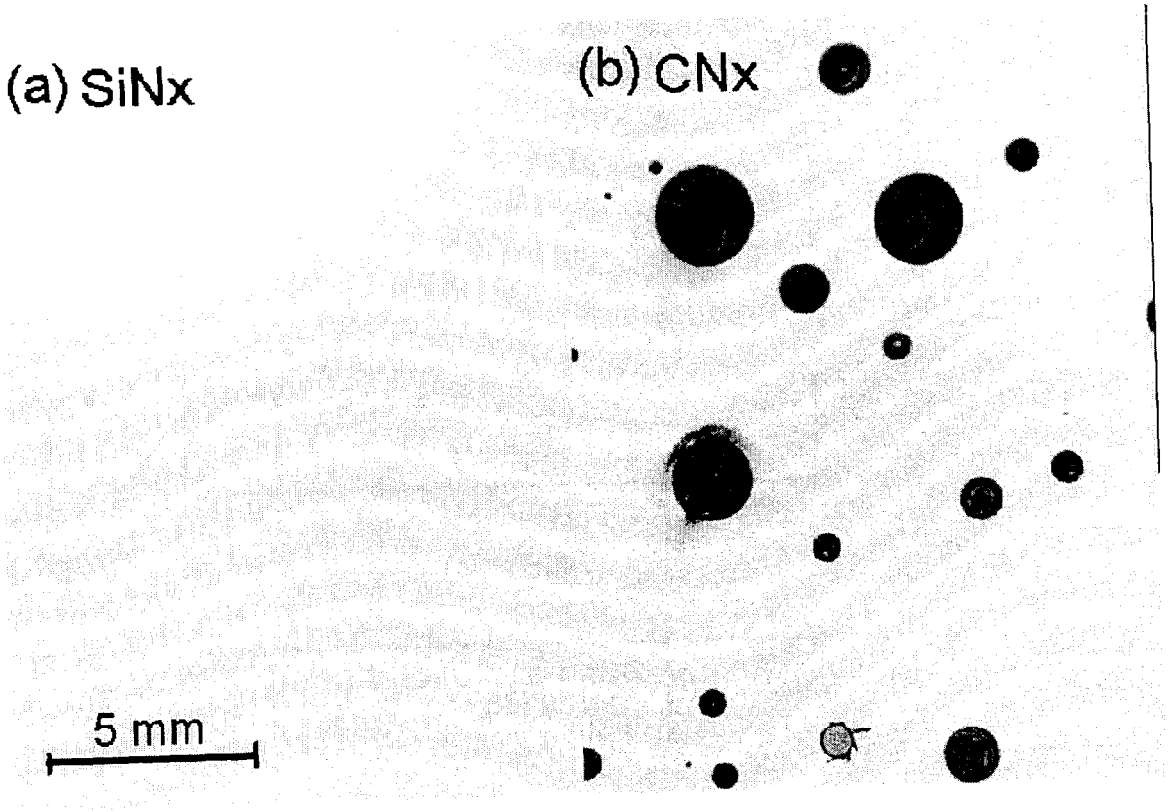

FIG. 13. Surfaces of CoPtCr disks coated with (a) 15 Å *a*-SiN_x and (b) 45 Å *a*-CN_x after 3 min etch in $Ce(NH_4)_2(NO_3)_6$ solution.

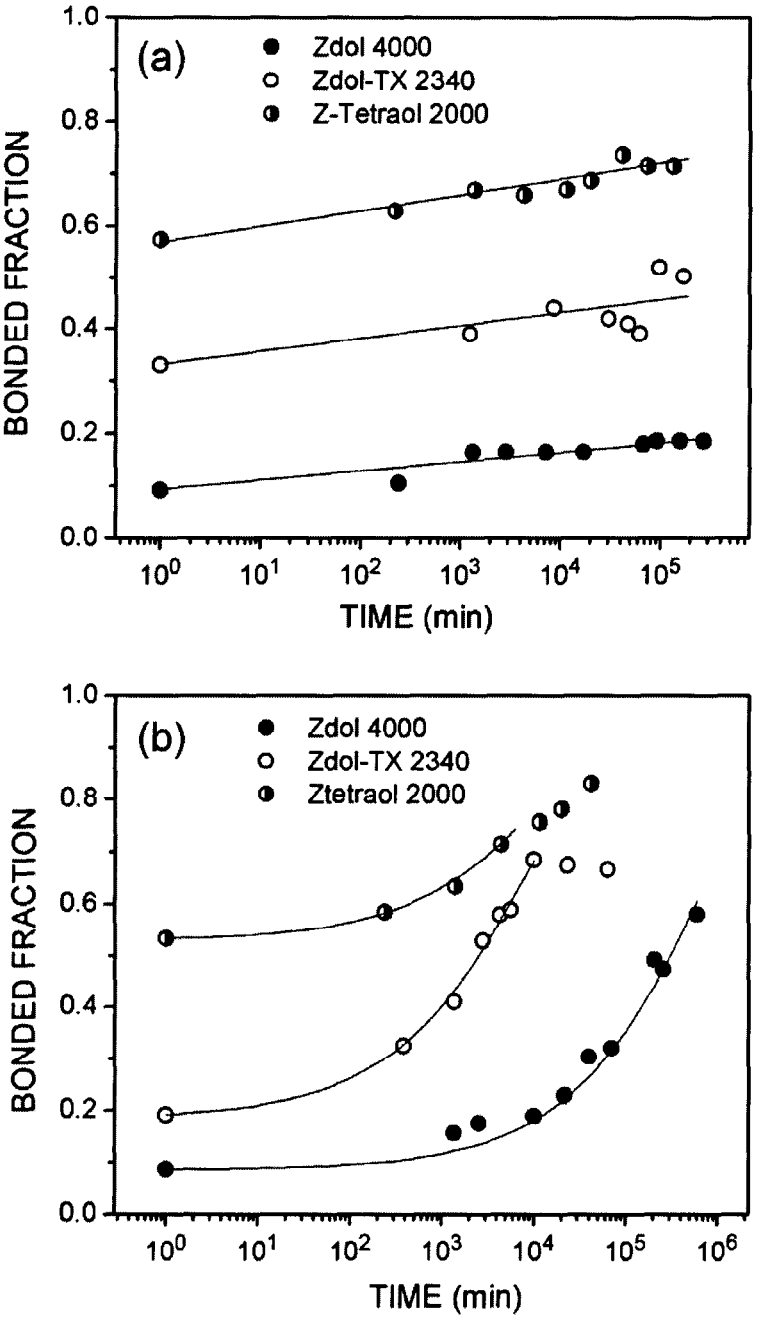

FIG. 14. Changes in the bonded fractions of Zdol 4000, Zdol-TX 2200, and Z-Tetraol 2200, on (a) *a*-SiN_x and (b) *a*-CN_x coated disks as a function of time at 21 °C and 50 ± 10% relative humidity. The initial lubricant film thicknesses are 13.0 ± 0.5 Å and 12.0 ± 0.5 Å for *a*-SiN_x and *a*-CN_x disks, respectively.

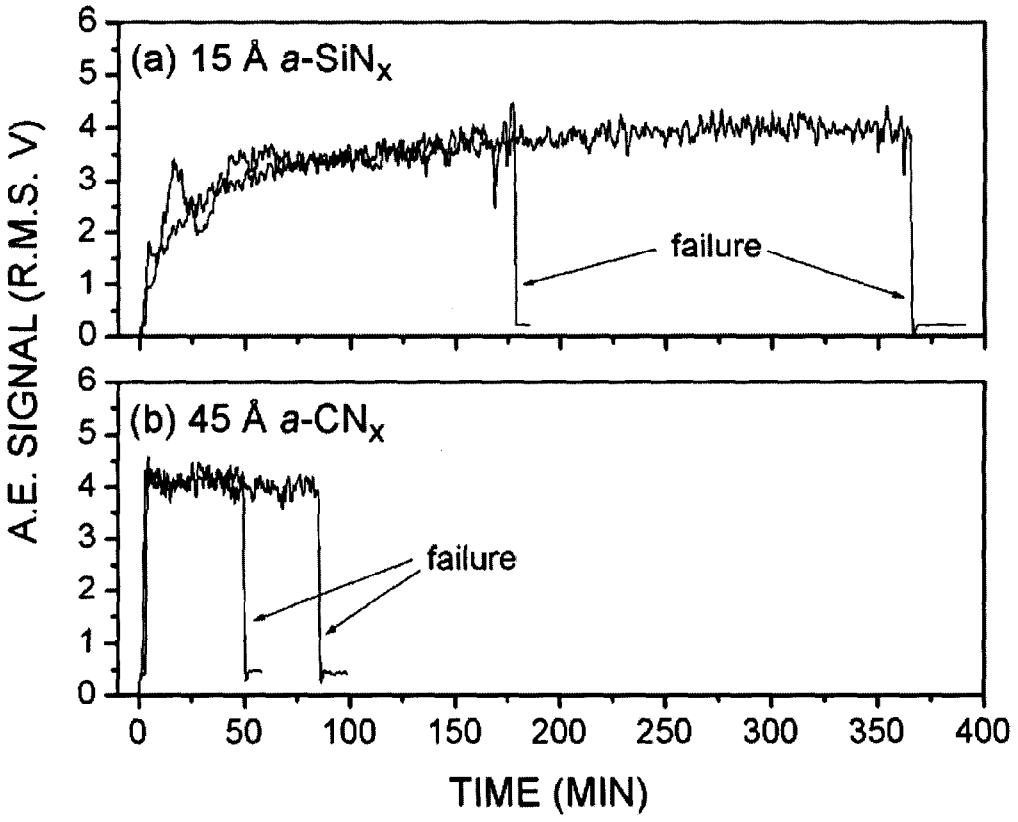

FIG. 15. Sample AE signals recorded during sub-ambient flyability test for (a) 15 Å a-SiN_x and (b) 45 Å a-CN_x coated disks.